Retinal Sublayer Thickness Analysis of The Macula of Symptomatic and Asymptomatic Carriers of G11778A Mutations with Leber's Hereditary Optic Neuropathy

Yufang Cheng
Eye Center, Renmin Hospital of Wuhan University, Wuhan 430060
Qingmei Miao
Eye Center, Renmin Hospital of Wuhan University, Wuhan 430060
Hongmei Zheng
Eye Center, Renmin Hospital of Wuhan University, Wuhan 430060
Lu He
Physical Examination Center, Renmin Hospital of Wuhan University, Wuhan 430060
Jiajia Yuan
Eye Center, Renmin Hospital of Wuhan University, Wuhan 430060
Changzheng Chen (whuchenchzh@163.com)
Eye Center, Renmin Hospital of Wuhan University, Wuhan 430060

Research Article

Keywords: Leber hereditary optic neuropathy, Optic neuropathy, Mitochondrial disorders, Optical coherence tomography, Thickness

Posted Date: March 18th, 2022

DOI: https://doi.org/10.21203/rs.3.rs-1454379/v1

Abstract

Background

Leber's hereditary optic neuropathy (LHON) is a maternally inherited mitochondrial genetic disease, caused mainly by *G11778A* mutations. Analysis of retinal sublayer structure by spectral domain optical coherence tomography(SD-OCT) is of great significance for elucidating the pathogenesis of LHON.

Purpose

To analyze the thicknesses of the outer plexiform layer (OPL), outer nuclear layer (ONL), photoreceptor inner and outer segment (IS/OS), and macula thickness (MT) in symptomatic and asymptomatic carriers of G11778A mutants with LHON using SD-OCT.

Methods

In this cross-sectional study, a total of 70 symptomatic carriers with the G11778A mutation were enrolled in Renmin Hospital of Wuhan University. Family members of symptomatic carriers were recruited as asymptomatic carriers for a final total of 36 participants. We also recruited 29 age- and sex-matched normal subjects.

Results

MT of symptomatic carriers was thinner than for asymptomatic carriers, while asymptomatic carriers were thinner than normal subjects. In carriers of the G11778A mutation, OPL thickness was increased, and ONL thickness was decreased compared to normal cases. Correlation analysis showed that MT was significantly correlated with peripapillary retinal nerve fiber layer (pRNFL) and disease duration, while ONL thickness in parafoveal nasal areas thinned as the disease progressed. The three groups showed no significant differences in IS/OS thicknesses.

Conclusions

The thicknesses of OPL, ONL and MT differed between normal subjects and symptomatic and asymptomatic carriers of G11778A mutations with LHON. MT and ONL thinning, in addition to OPL thickening, were observed in symptomatic and asymptomatic carriers, a finding which should be further validated and explored in basic science research. Additional longitudinal studies are needed to determine the usefulness of these findings to the diagnosis and monitoring of LHON.

Background

Leber's hereditary optic neuropathy (LHON) is a maternally inherited mitochondrial genetic disease. It causes bilateral acute (or subacute), painless loss of central vision in otherwise healthy young adults, especially men. More than 95% of LHON cases are caused by three point mutations in mitochondrial DNA (mt DNA), *G3460A, G11778A* and *T14484C*, of which the most common is *G11778A*. (1, 2) The *G11778A* mutation exhibits incomplete penetrance, so triggering of the pathological process may require additional genetic or environmental factors. To date, there are no methods to predict whether and when asymptomatic carriers will develop into symptomatic carriers (3). In this study, clinical and genetic criteria were used to divide subjects with the *G11778A* mutation into two groups: symptomatic carriers and asymptomatic carriers. All of the symptomatic carriers with LHON exhibited severe visual impairment. Asymptomatic carriers were defined as members of families with LHON who carried the *G11778A* mitochondrial mutation but had normal visual function, including visual acuity, color vision, and visual fields. As shown in numerous studies, visual loss in symptomatic carriers is mainly associated with apoptotic degeneration of retinal ganglion cells (RGCs) and their axons,(4) which has been supported by electrophysiological and histological studies.(5–7) However, the characteristic field defect of LHON is a central or paracentral scotoma,(8) and approximately 50% of RGCs are present in the macula. Therefore, evaluating structural changes in the macula is important for understanding the natural history and pathogenesis of LHON.

Optical coherence tomography (OCT) is a sensitive, reproducible and specific technique that can quantify retinal structures at micrometer scale, making it highly advantageous for monitoring retinal structural changes in LHON.(9) Zhang et al (10) were the first to use cirrus HD-OCT to quantify macular thicknesses (MT) in 52 symptomatic carriers. They classified symptomatic carriers based on disease duration and compared the degree of thinning between MT and peripapillary retinal nerve fiber layer (pRNFL). Byron et al (11) studied 20 symptomatic carriers, 31 asymptomatic carriers and 14 normal subjects, all of whom were subjected to macular cube scans with Cirrus OCT. They manually segmented the retina into six layers: retinal nerve fiber layer (RNFL), ganglion cell layer and inner plexiform layer (GCL + IPL), inner nuclear layer and outer plexiform layer (INL + OPL), photoreceptor outer segment (OS) and choroid. Thicknesses of macular sublayers were compared across the three groups, and their results showed no significant differences between asymptomatic carriers and normal subjects. Their findings showed that OS thickness was thicker in symptomatic carriers than in asymptomatic carriers and normal subjects. Inconsistent with their results, however, Wang et al (12) compared macular sublayer thicknesses of symptomatic carriers, asymptomatic carriers and normal subjects using RTVue100 OCT. OCT images were automatically segmented, and it was found that MT, GCL + IPL, and INL + OPL were all thickened in asymptomatic carriers, although the outer retina layer (ORL) was thinned. In addition, their results showed that the ORL of symptomatic carriers was thickened, consistent with the trend reported by Byron et al. However, the retinal layers they studied were inconsistent, so it remained unclear exactly which layers were thickened or thinned. Therefore, further stratification analysis of the macular retina in symptomatic carriers and asymptomatic carriers is critical. Until now, there have been no studies analyzing changes in macular OPL, ONL, and IS/OS thicknesses in symptomatic carriers and asymptomatic carriers. Moreover, compared with other OCT approaches, Spectralis OCT is more sensitive in detecting microstructural

changes and allows more accurate retinal stratification.(13, 14) Therefore, we performed improved retinal imaging using Spectralis OCT and compared the thicknesses of OPL, ONL, IS/OS and MT between symptomatic carriers and asymptomatic carriers of the *G11778A* mutation with LHON.

Methods

Participants

This study was performed at the Eye Center at Renmin Hospital of Wuhan University. A total of 70 symptomatic carriers were recruited from those diagnosed with m.*G11778A* mutation by genetic testing between February 2021 and October 2021 at Renmin Hospital of Wuhan University, China. Recruitment criteria: 1) age from 12 to 55 years; 2) painless visual loss in one or both eyes with central scotoma or paracentral scotoma; 3) genetically proven pure m.*G11778A* mutation with LHON; 4) intraocular pressure (IOP) < 21 mmHg; 5) no clinical evidence of any maculopathy during enrollment and follow-up; 6) clear OCT images. Exclusion criteria: 1) presence of glaucoma, ischemic optic neuropathy and other neuro ophthalmological diseases; 2) other ocular diseases affecting the cornea, lens, or retina; 3) severe physical illness; 4) poor subject fixation, leading to a low quality of the obtained images and a lack of cooperation with the researcher.

A total of 36 family members of these LHON symptomatic carriers were recruited as the asymptomatic carriers group. Recruitment criteria: 1) mothers of symptomatic carriers with genetically proven pure m.G 11778a LHON mutation, mothers' siblings or symptomatic carriers' siblings; 2) best corrected visual acuity (BCVA) of 1.0 (0.0 LogMAR) in both eyes; 3) refractive error < ± 5D; 4) IOP≥21 mmHg; 5) no clinical evidence of any maculopathy during enrollment and follow-up; 6) clear OCT images; 7) no history of eye surgery, injury or any ocular diseases; 8) no severe physical illness.

In addition, we recruited 29 age- and sex-matched normal subjects from the Eye Center at Renmin Hospital of Wuhan University. Recruitment criteria: 1) healthy men or women, aged from 12 to 55 years; 2) BCVA of 1.0 (0.0 LogMAR) in both eyes; 3) no ophthalmological discomfort, refractive error < ± 5D; 4) IOP≥21 mmHg;5) no clinical evidence of any maculopathy during enrollment and follow-up; 6) clear OCT images; 7) no history of eye surgery, injury or any ocular diseases; 8) no severe physical illness.

General Information

Patient age, gender, LHON duration, treatment experience and family history were collected, Both eyes of all symptomatic carriers underwent complete ophthalmic examinations, including slit-lamp examination, BCVA, ophthalmoscopy, IOP, 30 − 2 Humphrey visual field, fundus photography, pattern and flash visual evoked potential (pVEP, fVEP), electroretinogram (ERG), and macular and optic disc spectral domain OCT (SD-OCT).

OCT Imaging

The macula and optic disc were imaged by Spectralis HRA-OCT (Heidelberg Engineering, Heidelberg, Germany). All examinations were performed by a trained examiner. The diameter of the optic disc scanning ring was 3.4 mm, the real-time automatic tracking function was used, and images with a signal intensity > 15 were retained. The mean pRNFL thicknesses were measured using the built-in software of Spectralis HRA-OCT. Peripapillary retinal nerve fiber layer thicknesses in the superior, nasal, temporal, inferior and average quadrants (SpRNFL, NpRNFL, TpRNFL, IpRNFL, GpRNFL) were analyzed in this study. The macula was imaged by a horizontal B-scan through the fovea, with the real-time automatic tracking function employed. Images were superimposed 100 times, and images with a signal intensity > 15 were retained.

Thicknesses Measurements

Image J software (version 1.53 k, National Institutes of Health, USA) was used to measure the thicknesses of each sublayer of the macula. The process was presented in Fig. 1. First, images were imported into Image J software and calibrated. Second, parafovea nasal and parafovea temporal areas were defined as 150um away from the fovea in the OCT images obtained by a horizontal B-scan through the fovea. Third, the macula was stratified into 5 layers according to previous studies on retinal sublayers:(11, 12, 15, 16) 1) RNFL, 2) OPL, 3) ONL (the distance between the internal limiting membrane (ILM) and the external limiting membrane (ELM)), 4) IS/OS, 5) MT (thickness between the inner limiting membrane and the retinal pigment epithelium: ILM-RPE). The thicknesses of OPL, ONL, IS/OS and MT were measured at the fovea, parafovea nasal and parafovea temporal. Finally, measurement values were exported to Excel. Analysis of OCT images was performed by an independent researcher, and poor-quality images were excluded.

Statistical Analysis

SPSS statistical software (version 25.0, SPSS Inc, Chicago, Illinois, USA) was used for statistical analysis. Categorical variables were expressed as frequencies and percentages. All measurements are expressed as mean ± standard deviation (M ± SD). One-way analysis of variance (ANOVA) was performed to compare variations in the quantitative data among symptomatic carriers, asymptomatic carriers and normal subjects. Pearson correlation analysis was used to determine correlations between macular sublayer thicknesses and disease duration, ERG, Humphrey visual fields, pRNFL, visual evoked potential (VEP) in each area of the symptomatic carriers. Results with a p-value less than 0.05 were considered significant.

Results

Demographic Data

A total of 70 symptomatic carriers with the *G11778A* mutation, 36 asymptomatic carriers, and 29 normal subjects were recruited, with detailed demographic data presented in Table 1. In the symptomatic carriers group, there were 63 (90%) male and 7 female participants, with a mean age of 22.26 ± 8.383 years;

disease duration ranged from 2 to 240 months, and the mean disease duration was 36.18 ± 47.63 months. BCVA was 0.6–2.3 LogMAR, and mean BCVA was 1.74 ± 0.44 LogMAR. Asymptomatic carriers included 1 male and 35 female participants, with a mean age of 40.67 ± 7.079 years. In the control group, there were 21 males and 8 females, with a mean age of 27.41 ± 5.865 years. There were no statistically significant differences in age between the three groups (P > 0.05).

Table 1
Demographic data

Group	Number (person)	Age(years)	Male (%)	LogMAR BCVA	Disease duration (months)
symptomatic carriers	70	22.2 ± 8.383	90	1.74 ± 0.44	36.18 ± 47.63
asymptomatic carriers	36	40.6 ± 7.079	2.8	0.0	-
Normal subjects	29	27.4 ± 5.865	72.4	0.0	-
LogMAR BCVA: logarithm of minimum angle of resolution best corrected visual acuity					

Macular OCT

Macular sublayer thicknesses among symptomatic carriers, asymptomatic carriers, and normal subjects are summarized and compared in Table 2, Fig. 2.

Fovea

The differences in foveal ONL thicknesses and MT between the three groups were statistically significant (F = 11.308 and 3.801; P = 0.000 and 0.024), and no statistical differences were detected in IS/OS thicknesses (F = 1.659, P = 0.193). Multiple comparisons showed that the ONL thicknesses of symptomatic carriers and asymptomatic carriers (91.67 ± 13.01 μm and 94.98 ± 16.00 μm) were significantly lower than those of normal subjects (102.56 ± 14.54 μm) (P = 0.000 and 0.01), whereas no statistically significant differences were detected between symptomatic carriers and asymptomatic carriers (P = 0.359). MT of the symptomatic carriers (216.00 ± 13.50 μm) was significantly thinner than that of normal subjects (222.61 ± 20.18 μm) (P = 0.029), whereas no significant differences were observed between symptomatic carriers and asymptomatic carriers or between asymptomatic carriers and normal subjects (P > 0.05).

Parafoveal Temporal

OPL, ONL and MT thicknesses in the parafovea temporal were significantly different between the three groups (F = 4.772, 9.914, and 96.063, P = 0.009, 0.000, and 0.000), while there were no significant differences in IS/OS thicknesses (F = 0.575, P = 0.575). Multiple comparisons analysis revealed that OPL thickness was significantly thicker in symptomatic carriers (39.70 ± 12.14 μm) than in normal subjects (34.06 ± 8.01 μm) (P = 0.009), but no statistically significant differences were observed between

symptomatic carriers and asymptomatic carriers or between asymptomatic carriers and normal subjects (P > 0.05). ONL thicknesses were significantly thinner in symptomatic carriers and asymptomatic carriers (62.32 ± 14.59 μm and 60.33 ± 14.11 μm) compared to normal subjects (71.09 ± 14.27 μm),while there were no significant differences between symptomatic carriers and asymptomatic carriers or between asymptomatic carriers and normal subjects (P > 0.05). MT of symptomatic carriers (297.96 ± 25.05 μm) was significantly thinner than that of asymptomatic carriers (334.78 ± 28.20 μm), while that of asymptomatic carriers (334.78 ± 28.20 μm) was significantly thinner than that of normal subjects (362.19 ± 40.95 μm) (P = 0.000, 0.000, and 0.000).

Parafoveal Nasal

The thicknesses of OPL, ONL, IS/OS and MT in the parafoveal nasal differed across the three groups (F = 4.157, 9.838, 3.458, and 138.173; P = 0.017, 0.000, 0.033, and 0.000). Multiple comparisons testing indicated that OPL thicknesses of both symptomatic carriers and asymptomatic carriers (37.87 ± 9.95 μm and 39.62 ± 17.94 μm) were significantly increased compared to normal subjects (33.48 ± 6.34 μm) (P = 0.078, 0.016), while there were no statistically significant differences between symptomatic carriers and asymptomatic carriers (P > 0.05). ONL thicknesses of asymptomatic carriers (62.48 ± 16.70 μm) were significantly thinner than those of symptomatic carriers (69.82 ± 13.29 μm) (P = 0.002) and those of normal subjects (73.33 ± 13.79 μm) (P = 0.000), ONL thicknesses of symptomatic carriers (69.82 ± 13.29 μm) and normal subjects (73.33 ± 13.79 μm) were not significantly different (P = 0.395). The IS/OS thicknesses of symptomatic carriers (75.10 ± 6.68 μm) were significantly thicker than those of asymptomatic carriers (72.16 ± 6.18 μm) (P = 0.028), whereas there were no statistically significant differences between symptomatic carriers (75.10 ± 6.68 μm) and normal subjects (74.28 ± 10.46 μm) or between asymptomatic carriers (72.16 ± 6.18 μm) and normal subjects (74.28 ± 10.46 μm) (P > 0.05). MT of symptomatic carriers and asymptomatic carriers (310.25 ± 22.28 μm and 358.34 ± 29.56 μm) was significantly thinner than that of normal subjects (389.29 ± 46.83 μm) (P = 0.000 and 0.000), and MT of symptomatic carriers (310.25 ± 22.28 μm) was also significantly thinner than that of asymptomatic carriers (358.34 ± 29.56 μm) (P = 0.000).

Table 2
Comparison of macula sublayer thicknesses on OCT between symptomatic carriers, asymptomatic carriers and normal subjects (μm, M ± SD)

Macular thicknesses		Symptomatic Carriers	Asymptomatic Carriers	Normal Subjects	P#
Fovea	ONL	91.67 ± 13.01**	94.98 ± 16.00***	102.56 ± 14.54	0.000
	IS/OS	91.87 ± 7.35	92.24 ± 6.65	90.06 ± 7.40	0.193
	MT	216.00 ± 13.50**	220.06 ± 15.66	222.61 ± 20.18	0.024
Parafoveal temporal	OPL	39.70 ± 12.14**	36.72 ± 13.27	34.06 ± 8.01	0.009
	ONL	62.32 ± 14.59**	60.33 ± 14.11***	71.09 ± 14.27	0.000
	IS/OS	75.24 ± 8.29	73.97 ± 8.32	74.65 ± 7.74	0.575
	MT	297.96 ± 25.05*;**	334.78 ± 28.20***	362.19 ± 40.95	0.000
Parafoveal nasal	OPL	37.87 ± 9.95**	39.62 ± 17.94***	33.48 ± 6.34	0.017
	ONL	69.82 ± 13.29*	62.48 ± 16.70***	73.33 ± 13.79	0.000
	IS/OS	75.10 ± 6.68*	72.16 ± 6.18	74.28 ± 10.46	0.033
	MT	310.25 ± 22.28*;**	358.34 ± 29.56***	389.29 ± 46.83	0.000

OPL: outer plexiform layer, ONL: outer nuclear layer, IS/OS: photoreceptor inner and outer segment, MT: macula thickness; #: One way ANOVA; *: P < 0.05 between symptomatic carriers and asymptomatic carriers; **: P < 0.05 between symptomatic carriers and controls; ***: P < 0.05 between asymptomatic carriers and controls.

Correlation Analysis

LogMAR BCVA of symptomatic carriers was negatively correlated with VFI, MD (r = -0.475 and − 0.495, P = 0.000 and 0.000), SpRNFL, IpRNFL and GpRNFL thicknesses (r = -0.179, -0.188, and − 0.226, P = 0.048, 0.039, and 0.012), PVEP 0 .5 and 1.0 cpd P100 amplitude (r = -0.340 and − 0.232; P = 0.000 and 0.010). Our findings are consistent with the findings of previous studies.(17, 18) For symptomatic carriers, there was no significant correlation between LogMAR BCVA and disease duration (r = -0.004, P = 0.963). Correlations between macula sublayer thicknesses (OPL, ONL, IS/OS, MT) and disease duration, PERG, visual field, and pRNFL thicknesses of symptomatic carriers are shown in Table 3.

Fovea

IS/OS thicknesses were negatively correlated with N95 (r = -0.253, P = 0.043) but positively correlated with time of FVEP, N2, and P2 wave (r = 0.280 and 0.223; P = 0.002 and 0.015). MT was positively correlated with SpRNFL, NpRNFL, IpRNFL and GpRNFL thicknesses (r = 0.190, 0.184, 0.275, and 0.217, P = 0.036, 0.043, 0.002, and 0.017).

Parafoveal Temporal

IS/OS thicknesses were negatively correlated with N95 and amplitude of FVEP (r = -0.260 and − 0.225; P = 0.038 and 0.014). MT was negatively correlated with disease duration (r = -0.240, P = 0.007), positively correlated with P50, VFI, and MD (r = 0.364, 0.226, and 0.225; P = 0.003, 0.013, and 0.014), and positively correlated with SpRNFL, NpRNFL, IpRNFL, TpRNFL, and GpRNFL thicknesses (r = 0.290, 0.327, 0.353, 0.330, and 0.349; P = 0.001, 0.000, 0.000, and 0.000, respectively).

Parafoveal Nasal

OPL thicknesses were positively correlated with P50 (r = 0.267, P = 0.035). ONL thicknesses were negatively correlated with disease duration and 0.5 cpd PVEP (r = -0.210 and − 0.232; P = 0.019 and 0.010, respectively). IS/OS thicknesses and 2.0cpd PVEP were negatively correlated with one another (r = -0.183, P = 0.043) but positively correlated with FVEP (r = 0.249, P = 0.007). MT was negatively correlated with disease duration (r = -0.179, P = 0.047) but positively correlated with IpRNFL, TpRNFL and GpRNFL thicknesses (r = 0.214, 0.327, and 0.186, P = 0.018, 0.000, and 0.040). In addition, MT was negatively correlated with 2.0cpd PVEP (r = -0.178, P = 0.049) but positively correlated with time of FVEP (r = 0.225, P = 0.007).

Table 3. Correlations between macula sublayer thicknesses and disease duration, PERG, visual field, and pRNFL in symptomatic carriers

Correlation Analysis/R		Disease Duration	LogMARBCVA	P50	N95	VFI	MD	SpRNFL	NpRNFL	IpRNFL	TpRNFL	GpRNFL
Fovea	ONL	-0.103	0.049	0.177	-0.097	-0.017	-0.015	0.158	0.13	0.173	0.025	0.15
	IS/OS	-0.087	-0.076	0.096	-.253*	0.013	0.027	0.038	0.009	0.069	0.176	0.031
	MT	-0.164	-0.019	0.186	-0.225	-0.003	0.009	.190*	.184*	.275**	0.144	.217*
	OPL	0.129	0.017	0.047	-0.113	-0.029	-0.016	-0.108	0.118	-0.029	0.019	-0.032
Parafoveal Temporal	ONL	-0.096	0.147	0.094	-0.136	-0.056	-0.084	0.104	0.029	0.033	0.032	0.084
	IS/OS	-0.036	-0.07	0.198	-.260*	0.089	0.1	0.114	0.164	0.148	0.156	0.146
	MT	-.240**	0.033	.364**	-0.195	.226*	.225*	.290**	.327**	.353**	.330**	.349**
	OPL	0.133	-0.032	.267*	0.07	0.148	0.173	0.014	0.156	0.069	0.013	0.084
Parafoveal Nasal	ONL	-.210*	0.136	-0.209	-0.128	-0.075	-0.104	-0.002	-0.077	-0.051	0.064	-0.049
	IS/OS	-0.103	0.041	-0.111	-0.171	-0.033	-0.025	0.012	-0.041	0.009	0.166	-0.019
	MT	-.179*	0.019	-0.017	-0.125	0.053	0.053	0.172	0.084	.214*	.327**	.186*

*: P < 0.05; **: P < 0.01; LogMAR BCVA: logarithm of minimum angle of resolution best corrected visual acuity; P50, N95: pattern electroretinogram P50, N95 waves; VFI: visual field index; MD: mean defect; SpRNFL, NpRNFL, TpRNFL, IpRNFL, GpRNFL: peripapillary retinal nerve fiber layer thicknesses in the superior, nasal, temporal, inferior and average quadrants.

Discussion

This study used Spectralis HRA-OCT to investigate macula sublayer thicknesses in the fovea and parafovea of symptomatic carriers and asymptomatic carriers of the *G11778A* mutation with LHON. We compared characteristics of macula sublayer thicknesses between symptomatic carriers, asymptomatic

carriers and normal subjects. In addition, we further analyzed the correlations between macula sublayer thickness and disease duration, PERG, visual fields, pRNFL, and VEP in symptomatic carriers.

Previous studies of MT have concluded that MT is thinner in symptomatic carriers compared to asymptomatic carriers and normal subjects, and no statistically significant differences have been reported between MT of asymptomatic carriers and normal subjects.(10–12) In our study, we also found MT thinning in symptomatic carriers. Furthermore, our study identified thinning in the parafoveal temporal and nasal areas and determined that MT of asymptomatic carriers is significantly thinner than that of normal subjects, in agreement with the trends of previous studies.(11, 12) However, those studies failed to report any statistically significant differences, potentially due to their small sample sizes. Correlation analysis showed that thinning in the MT and parafoveal temporal and nasal regions is correlated with pRNFL and disease duration in symptomatic carriers. This correlation indicates that the symptomatic carriers we recruited were at an advanced stage of LHON, and MT of symptomatic carriers was thinning as LHON progressed. In the parafoveal nasal area, MT thinning was also correlated with P50, VFI, and MD, further revealing a tendency for structural changes to coincide with changes in indices of visual function. It remains to be conclusively determined whether the range of structural changes corresponds with changes in visual function.

The OPL, the first synapse of the visual system ,is formed jointly by cone and rod photoreceptors in the ONL and horizontal cells (HCs) and bipolar cells (BCs) in the INL.(19) Some animal studies (3, 20) have shown that BCs and their synapses exhibit a certain amount of plasticity, with the number of BCs increasing soon after cutting of the optic nerve. In this case, we speculate that RGCs underwent apoptosis similar to that which occurred after optic nerve severance. The loss of RGCs could stimulate an increase in the number of BCs, in turn causing the OPL to become thicker. Byron L and Huang et al (11, 12) both analyzed the thicknesses of the INL + OPL. Byron L et al did not find significant differences between the three groups, while Huang et al found that both symptomatic and asymptomatic carriers had thicker INL + OPL thicknesses in most regions than the control group. In our study, we also found that macular OPL thicknesses were significantly increased in symptomatic carriers and asymptomatic carriers compared to normal subjects (except for the parafoveal temporal area of asymptomatic carriers, $P > 0.05$), consistent with Huang et al. Our correlation analysis showed that in symptomatic carriers, OPL thickness is significantly correlated with P50 in the parafoveal nasal region, further indicating that OPL thickening may be related to RGC apoptosis.

Our study demonstrated that ONL thicknesses were thinner in both symptomatic carriers and asymptomatic carriers compared to normal subjects. In addition, ONL thicknesses in the parafoveal nasal region were thinner in asymptomatic carriers than in symptomatic carriers. Correlation analysis shows that ONL thickness in the parafoveal nasal region becomes thinner with disease duration. Partially contrary to our findings, Byron L et al (11) reported that the ONL + IS thickness of symptomatic carriers was thicker than that of normal subjects. Consistent with some of our findings, thicknesses of the ONL + IS were thinner in asymptomatic carriers than in symptomatic carriers ($P > 0.05$). The reasons for these inconsistencies may be due to two factors: 1) the analysis may be altered by a superimposition effect,

such as that observed when Fan et al(21) studied glaucomatous disease and found that the foveal ONL was significantly thickened in glaucomatous eyes; however when combining the three sublayers (ONL + IS + OS), no significant differences were observed between glaucoma patients and controls;2) measurements of the ONL layer may be influenced by the Helen fiber layer.(22) Until now, no studies have described the ONL layer in symptomatic carriers with LHON. Recently, Fujihara et al(23) published a study on glaucoma that found significant thinning of the ONL in advanced open-angle glaucoma. It has also been reported that macular ONL thickness increases in the early stages of glaucoma, then gradually thins in the later stages until the thickness approached that of normal subjects.(21) At the parafovea, ONL thicknesses in glaucoma was not significantly different from normal subjects.(24) Glaucoma, like LHON, involves damage to both RGCs and their axons, leading to progressive thinning of the GCL and RNFL. Therefore, we suspect that the mechanisms by which these two diseases lead to ONL thinning may be consistent. Pathologic studies of glaucoma have identified that thickening of the foveal ONL may be associated with enlarged cone nuclei and swollen somata.(25) The cause of ONL thinning remains uncertain at present; studies with large sample sizes and prospective studies are needed in the future to explore the mechanisms by which ONL thicknesses are changed, the pathogenesis of ONL thinning and RGC apoptosis.

In our study, there were no significant differences in IS/OS thicknesses between carriers with the *G11778A* mutation and normal subjects. IS/OS thicknesses in the parafoveal nasal region of symptomatic carriers were significantly thicker than those of asymptomatic carriers. Correlation analysis identified significant correlations between IS/OS thicknesses in foveal and parafoveal temporal areas and N95 amplitude, FVEP P2 amplitude, and wave time. Byron L et al (11) analyzed the OS layer alone and found that thickness of the OS layer was significantly increased in symptomatic carriers compared to asymptomatic carriers and normal subjects. Histological studies of patients with LHON (5, 6) have shown that photoreceptors and RPE are unaffected; however, it may be histologically difficult to clarify the cause of mild OS thickening. Huang et al (12) analyzed ONL + IS + OS + RPE thicknesses and found that symptomatic carriers were significantly thicker than asymptomatic carriers. There were difficulties in differentiating the outer retinal structures by OCT, as there was no uniformity in the stratification of the outer layers of the retina. In this study, IS/OS thicknesses were significantly correlated with PERG and VEP, indicating that IS/OS stratification of the outer layer of the retina can reflect its functional index to some extent.

The limitations of this study include: 1) to date, we have not been able to complete a longer follow-up study of LHON patients; 2) in order to obtain clear Spectralis HRA-OCT images, a single-line B-scan mode was used in this study; 3) the thickness of each sublayer was measured using manual marker points; 4) did not perfect the correlation analysis of asymptomatic carriers and normal subjects; 5) differences in the ages of symptomatic carriers and asymptomatic carriers. Future longitudinal studies with larger sample sizes will be conducted to further understand the natural history and pathogenesis of LHON.

Conclusion

In conclusion, we analyzed the foveal and parafoveal sublayer thicknesses of symptomatic and asymptomatic carriers of the *G11778A* mutation with LHON in comparison to normal subjects using Spectralis HRA-OCT. Our study showed that the thicknesses of OPL, ONL, IS/OS and MT differed across the three groups. Macular sublayer thickness analysis was useful in distinguishing between normal subjects and carriers of *G11778A* mutations with LHON. MT and ONL thinning, as well as OPL thickening, were detected in symptomatic and asymptomatic carriers, which should be further validated and explored in basic science research. Future longitudinal studies are needed to determine the usefulness of these measurements in the diagnosis and monitoring of LHON.

Declarations

Ethics approval and consent to participate

This study was conducted according to the guidelines of the Declaration of Helsinki and approved by the Clinical Research Ethics Committee of Renmin Hospital of Wuhan University (WDRY2021-K018). Written informed consent was obtained from all participants.

Consent for publication

Not applicable

Availability of data and materials

The data presented in this study are available on request from the corresponding author.

Competing interests

The authors declare that they have no competing interests.

Funding:

This work was supported by the National Natural Science Foundation of China (Grant No.82101115) and Wuhan University Independent Innovation Fund Youth Project（Grant No.2042021kf0094）. The funders had no role in the design of the study, in the collection, analyses, or interpretation of data; in the writing of the manuscript; or in the decision to publish the results.

Authors' Contributions

Conceptualization, Y.F.C., C.Z.C. and J.J.Y.; methodology, Y.F.C., C.Z.C. and H.M.Z.; formal analysis, Y.F.C., C.Z.C. , Q.M.M., H.M.Z. and J.J.Y.; investigation, Y.F.C., C.Z.C., Q.M.M.,H.M.Z. ,L.H and J.J.Y.; project administration, Y.F.C., C.Z.C., H.M.Z., L.H. and J.J.Y.; resources, C.Z.C., H.M.Z., L.H. and J.J.Y.; software, Y.F.C.; supervision, C.Z.C. and H.M.Z.; validation, Y.F.C. and C.Z.C.; Visualization Y.F.C. and C.Z.C.; data curation, Y.F.C.; writing—original draft, Y.F.C. and C.Z.C.; writing—review and editing, Y.F.C., C.Z.C. and H.M.Z. All authors have read and agreed to the published version of the manuscript.

Acknowledgements

We thank the participants and study staff and Renmin Hospital of Wuhan University for their contributions to the study.

References

1. Kerrison JB, Newman NJ. Clinical spectrum of Leber's hereditary optic neuropathy. Clin Neurosci. 1997;4(5):295–301.
2. Mashima Y, Yamada K, Wakakura M, Kigasawa K, Kudoh J, Shimizu N, et al. Spectrum of pathogenic mitochondrial DNA mutations and clinical features in Japanese families with Leber's hereditary optic neuropathy. Curr Eye Res. 1998;17(4):403–8.
3. Germain F, Fernandez E, de la Villa P. Morphometrical analysis of dendritic arborization in axotomized retinal ganglion cells. Eur J Neurosci. 2003;18(5):1103–9.
4. Balducci N, Savini G, Cascavilla ML, La Morgia C, Triolo G, Giglio R, et al. Macular nerve fibre and ganglion cell layer changes in acute Leber's hereditary optic neuropathy. Br J Ophthalmol. 2016;100(9):1232–7.
5. Levin LA. Mechanisms of retinal ganglion specific-cell death in Leber hereditary optic neuropathy. Trans Am Ophthalmol Soc. 2007;105:379–91.
6. Kerrison JB, Howell N, Miller NR, Hirst L, Green WR. Leber hereditary optic neuropathy. Electron microscopy and molecular genetic analysis of a case. Ophthalmology. 1995;102(10):1509–16.
7. Ziccardi L, Sadun F, De Negri AM, Barboni P, Savini G, Borrelli E, et al. Retinal function and neural conduction along the visual pathways in affected and unaffected carriers with Leber's hereditary optic neuropathy. Invest Ophthalmol Vis Sci. 2013;54(10):6893–901.
8. Newman NJ, Biousse V, Newman SA, Bhatti MT, Hamilton SR, Farris BK, et al. Progression of visual field defects in leber hereditary optic neuropathy: experience of the LHON treatment trial. Am J Ophthalmol. 2006;141(6):1061–7.
9. Huang D, Swanson EA, Lin CP, Schuman JS, Stinson WG, Chang W, et al. Optical coherence tomography. Science. 1991;254(5035):1178–81.
10. Zhang Y, Huang H, Wei S, Gong Y, Li H, Dai Y, et al. Characterization of macular thickness changes in Leber's hereditary optic neuropathy by optical coherence tomography. BMC Ophthalmol. 2014;14:105.
11. Lam BL, Burke SP, Wang MX, Nadayil GA, Rosa PR, Gregori G, et al. Macular Retinal Sublayer Thicknesses in G11778A Leber Hereditary Optic Neuropathy. Ophthalmic Surg Lasers Imaging Retina. 2016;47(9):802–10.
12. Huang S, Chen Q, Ma Q, Liu X, Lu F, Shen M. THREE-DIMENSIONAL CHARACTERISTICS OF FOUR MACULAR INTRARETINAL LAYER THICKNESSES IN SYMPTOMATIC AND ASYMPTOMATIC CARRIERS OF G11778A MUTATION WITH LEBER'S HEREDITARY OPTIC NEUROPATHY. Retina. 2016;36(12):2409–18.

13. Mahmoudinezhad G, Mohammadzadeh V, Amini N, Delao K, Zhou B, Hong T, et al. Detection of Longitudinal Ganglion Cell/Inner Plexiform Layer Change: Comparison of Two Spectral-Domain Optical Coherence Tomography Devices. Am J Ophthalmol. 2021;231:1–10.
14. Mylonas G, Ahlers C, Malamos P, Golbaz I, Deak G, Schuetze C, et al. Comparison of retinal thickness measurements and segmentation performance of four different spectral and time domain OCT devices in neovascular age-related macular degeneration. Br J Ophthalmol. 2009;93(11):1453–60.
15. Matsumoto H, Sato T, Kishi S. Outer Nuclear Layer Thickness at the Fovea Determines Visual Outcomes in Resolved Central Serous Chorioretinopathy. American Journal of Ophthalmology. 2009;148(1):105–10.
16. Aboualizadeh E, Ranji M, Sorenson CM, Sepehr R, Sheibani N, Hirschmugl CJ. Retinal oxidative stress at the onset of diabetes determined by synchrotron FTIR widefield imaging: towards diabetes pathogenesis. Analyst. 2017;142(7):1061–72.
17. Barboni P, Carbonelli M, Savini G, Ramos Cdo V, Carta A, Berezovsky A, et al. Natural history of Leber's hereditary optic neuropathy: longitudinal analysis of the retinal nerve fiber layer by optical coherence tomography. Ophthalmology. 2010;117(3):623–7.
18. Hwang TJ, Karanjia R, Moraes-Filho MN, Gale J, Tran JS, Chu ER, et al. Natural History of Conversion of Leber's Hereditary Optic Neuropathy: A Prospective Case Series. Ophthalmology. 2017;124(6):843–50.
19. Mumm JS, Godinho L, Morgan JL, Oakley DM, Schroeter EH, Wong RO. Laminar circuit formation in the vertebrate retina. Prog Brain Res. 2005;147:155–69.
20. Germain F, Calvo M, de la Villa P. Rabbit retinal ganglion cell survival after optic nerve section and its effect on the inner plexiform layer. Exp Eye Res. 2004;78(1):95–102.
21. Fan N, Huang N, Lam DS, Leung CK. Measurement of photoreceptor layer in glaucoma: a spectral-domain optical coherence tomography study. J Ophthalmol. 2011;2011:264803.
22. Tong KK, Lujan BJ, Zhou Y, Lin MC. Directional Optical Coherence Tomography Reveals Reliable Outer Nuclear Layer Measurements. Optom Vis Sci. 2016;93(7):714–9.
23. Fujihara FMF, de Arruda Mello PA, Lindenmeyer RL, Pakter HM, Lavinsky J, Benfica CZ, et al. Individual Macular Layer Evaluation with Spectral Domain Optical Coherence Tomography in Normal and Glaucomatous Eyes. Clin Ophthalmol. 2020;14:1591–9.
24. Wygnanski T, Desatnik H, Quigley HA, Glovinsky Y. Comparison of ganglion cell loss and cone loss in experimental glaucoma. Am J Ophthalmol. 1995;120(2):184–9.
25. Nork TM, Ver Hoeve JN, Poulsen GL, Nickells RW, Davis MD, Weber AJ, et al. Swelling and loss of photoreceptors in chronic human and experimental glaucomas. Arch Ophthalmol. 2000;118(2):235–45.

Figures

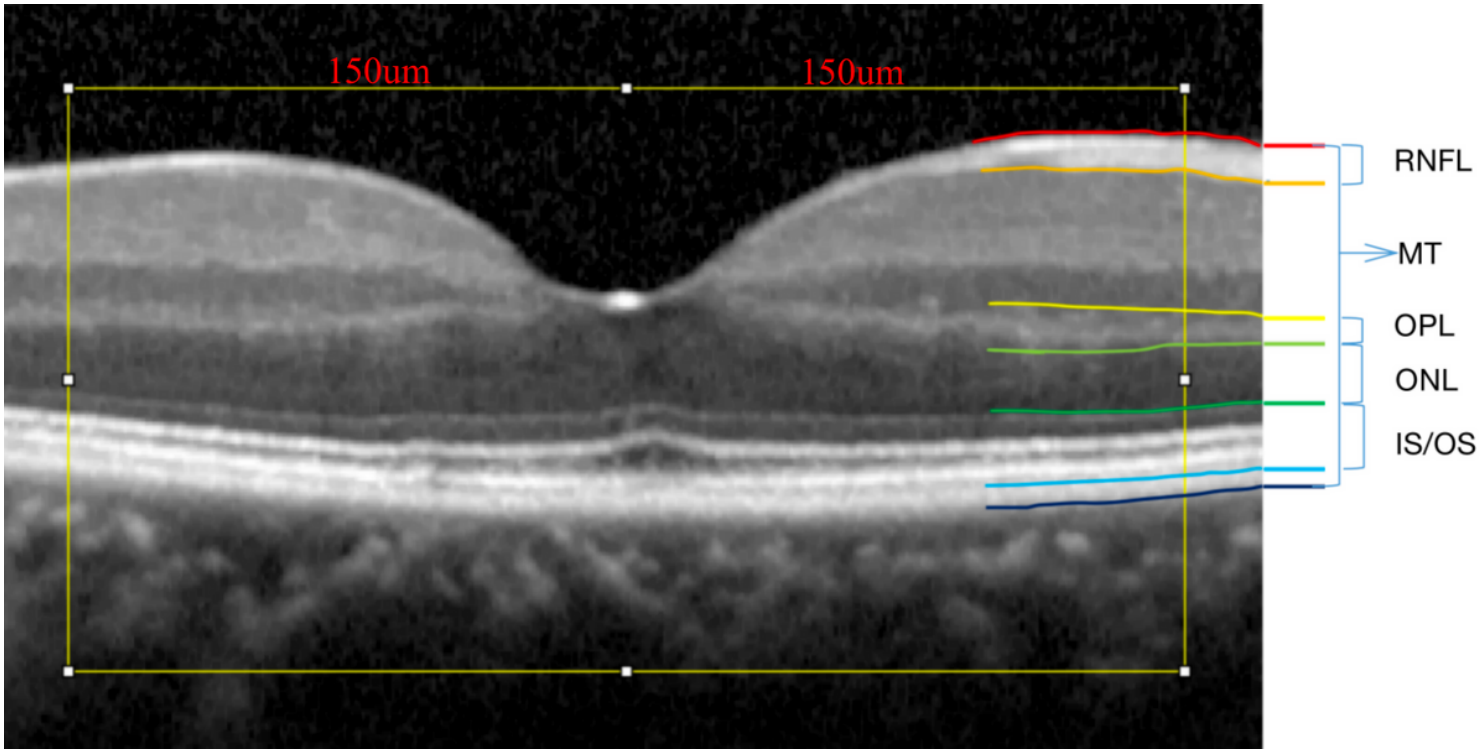

Figure 1

Retinal layering and methods of measurement. RNFL: retinal nerve fiber layer, OPL: outer plexiform layer, ONL: outer nuclear layer (the distance between the internal limiting membrane (ILM) and the external limiting membrane (ELM)), IS/OS: photoreceptor inner and outer segment, MT: macula thickness (thickness between the inner limiting membrane and the retinal pigment epithelium: ILM-RPE).

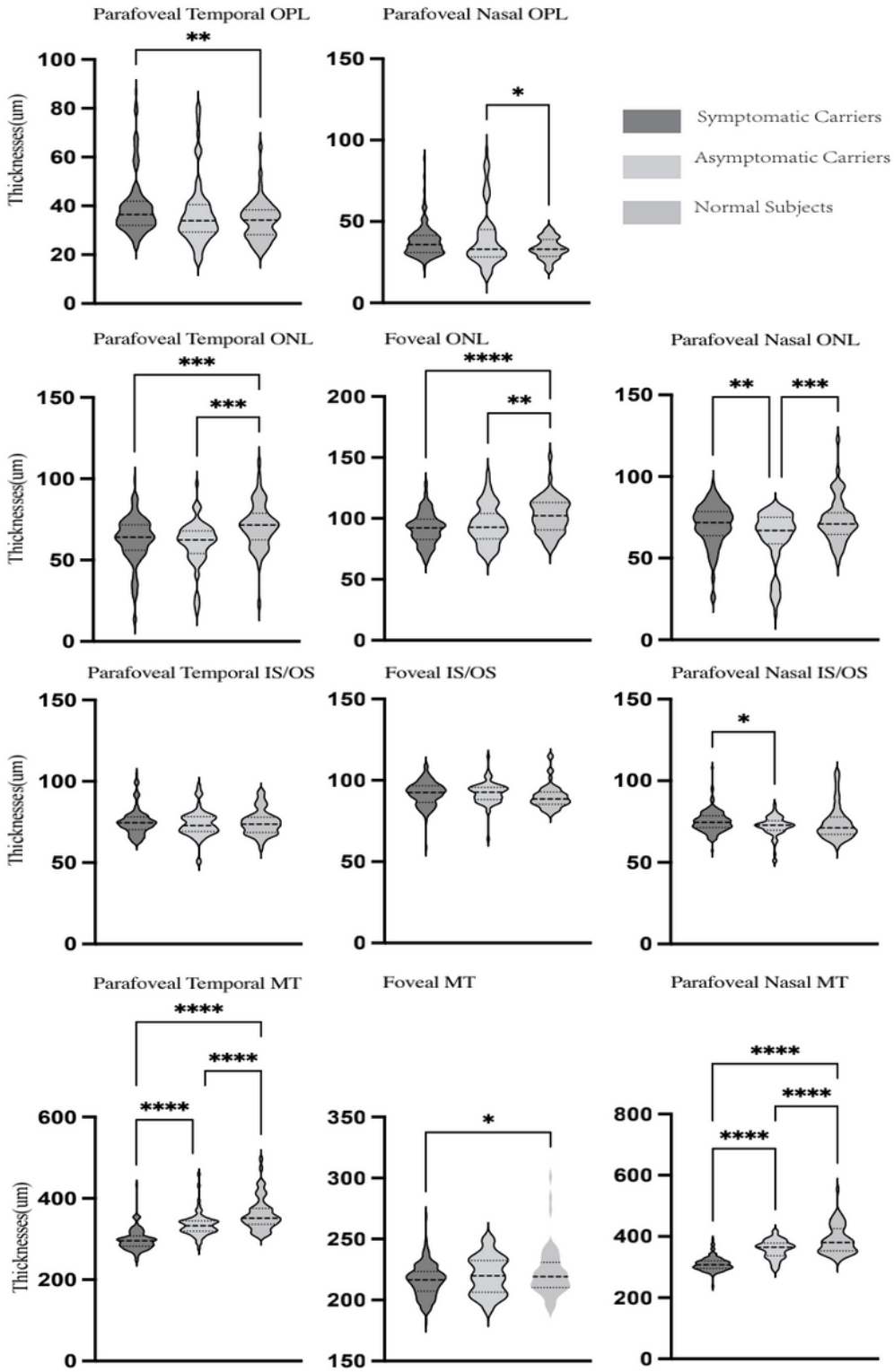

Figure 2

MT and Macular OPL, ONL, IS/OS thicknesses of symptomatic carriers, asymptomatic carriers of *G11778A* mutation with LHON and normal subjects. Bottom and top horizontal lines of each box represent 25th and 75th percentiles, respectively, and the middle line represents the 50th percentile, or median. The width of the graph represents the number of cases in this interval. OPL: outer plexiform layer,

ONL: outer nuclear layer, IS/OS: photoreceptor inner and outer segment, MT: macula thickness; *: P<0.0332, **: P<0.0021, ***: P<0.0002 , ****: <0.0001.